

Supporting Information for:
MrDNA: A multi-resolution model for predicting the
structure and dynamics of DNA systems

Christopher Maffeo^{1,2} and Aleksei Aksimentiev^{*,1,2}

¹ Department of Physics
University of Illinois at Urbana-Champaign
1110 W Green St, Urbana, IL 61801

² Beckman Institute for Advanced Science and Technology
University of Illinois at Urbana-Champaign
405 N Mathews Ave, Urbana, IL 61801

*To whom correspondence should be addressed. Tel: +1 217-333-6495; Email: aksiment@illinois.edu

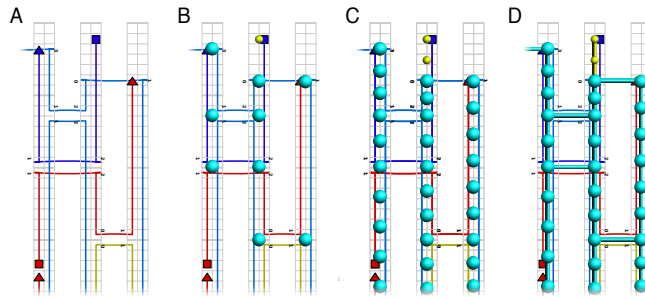


Figure S1: Schematic of bead placement algorithm. (A) First, splines run through the idealized coordinates provided from an input source, such as the *cadnano*¹ model shown here. (B) Double- and single-stranded beads (cyan and yellow spheres) are placed at the ends of and junctions between dsDNA and ssDNA regions. As beads are placed, they are merged into a single bead if placed below a user-specified threshold. (C) Beads are then placed to fill the space between those already placed. The beads are placed such that a user-specified density is not exceeded (shown here, 3 bp/bead and 3 nt/bead). (D) Finally, potentials are placed to connect the beads.

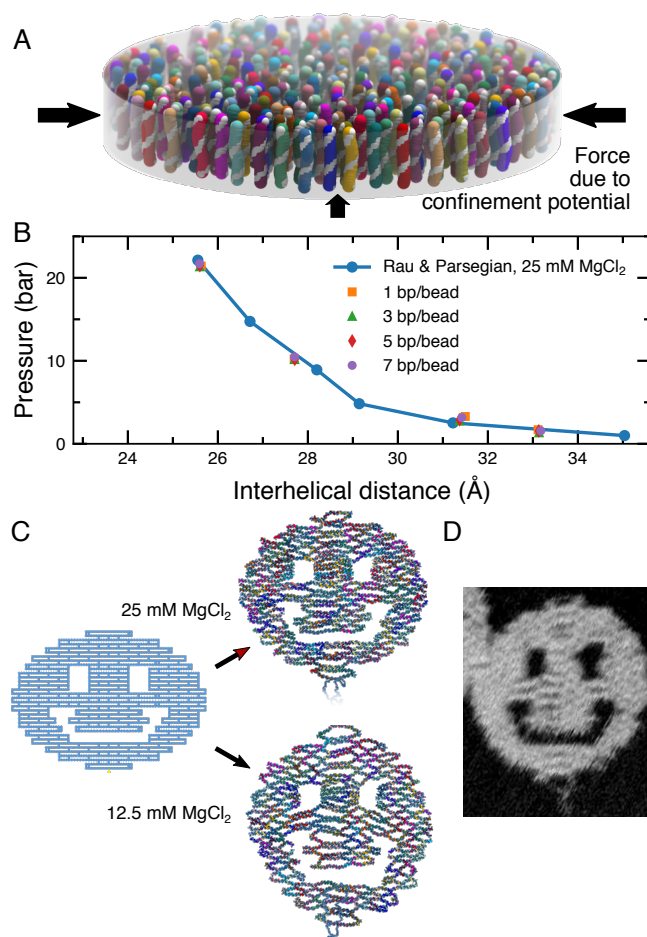


Figure S2: Calibration of non-bonded interactions. (A) Validation of the coarse-grained non-bonded potentials through simulations of a dsDNA array at several resolutions. The simulation system consists of 256 two-turn DNA helices with ends connected across a 6.4 nm periodic boundary confined by a cylindrical harmonic potential. The pressure within the array is measured by accumulating the force applied by the cylindrical potential. (B) Dependence of pressure on the DNA distance. The blue circles depict the experimentally derived pressure of a DNA array in 25 mM MgCl₂ solution as a function of the inter-DNA distance taken from Ref. 2. The colored symbols depict the pressure measured in *mrdna* simulations of 256 two-turn DNA helices at several resolutions. (C) The effect of ion concentration on the simulated structure of a two-dimensional DNA origami object. A cadnano file of the “smiley” object was produced according to the pattern described in the original manuscript.³ The *mrdna* model of the smiley was relaxed from its initial configuration (left) using the default description of interactions in a 25 mM MgCl₂ solution (top) and using a Debye-Hückel correction to match the experimental conditions of 12.5 mM MgCl₂ (bottom). The surface on which the smiley is deposited was modeled using a grid-based potential derived using the Derjaguin approximation for an infinite slab interacting with the DNA through a Lennard-Jones potential with $r_{\min} = 15.5 \text{ \AA}$ and $\epsilon = 0.1 \text{ kcal/mol}$. (D) Image of the smiley experimentally obtained using atomic force microscopy. Reproduced from Supplementary Figure S26 associated with Ref. 3.

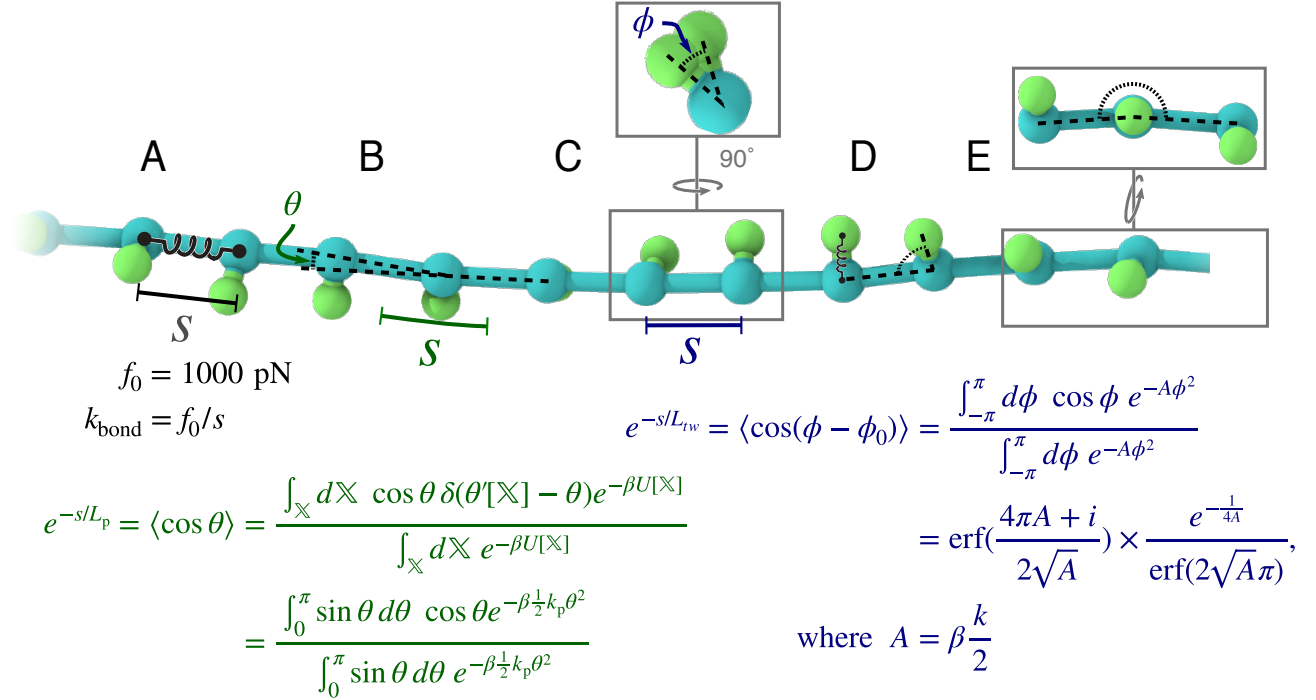


Figure S3: Schematic representation of bonded interactions in the `mrdna` model. (A) A harmonic spring connects adjacent beads with spring constant derived from the experimentally-determined elastic constant of dsDNA (1000 pN).⁴ (B) A harmonic spring applied to the angle between the bonds formed by adjacent pairs of beads has its spring constant numerically determined from the experimentally-determined persistence length of dsDNA (50 nm). The remaining terms are applied when twist is locally represented. (C) A harmonic spring is applied to the dihedral angle formed by each orientation bead, its parent dsDNA bead, the adjacent dsDNA bead and its orientation bead to reproduce a twist persistence length within the range of experimentally-obtained values (90 nm).⁵ (D) A harmonic bond associates each orientation bead with its dsDNA backbone bead (1.5 Å rest-length; $k_{\text{spring}} = 30 \text{ kcal/mol \AA}^2$); the orientation bond is kept roughly normal to the local tangent of the DNA by a harmonic angle potential with 90° rest angle and $k_{\text{spring}} = 0.25 k_{Lp}$; the backbone angle potential spring constant (schematically illustrated in panel B) is reduced by a factor of 0.75 to compensate for the added rigidity imparted by the orientation beads. (E) A harmonic potential applied to the improper dihedral angle formed by the bead below a dsDNA bead, the dsDNA bead, its orientation bead and the bead above the dsDNA bead provides additional stiffness in the direction normal to the bead axis to compensate for the loss of stiffness generated by reducing the spring constant of the angle potential (panel B). Black, green and blue equations correspond to the potentials described in panels A, B and C, in that order.

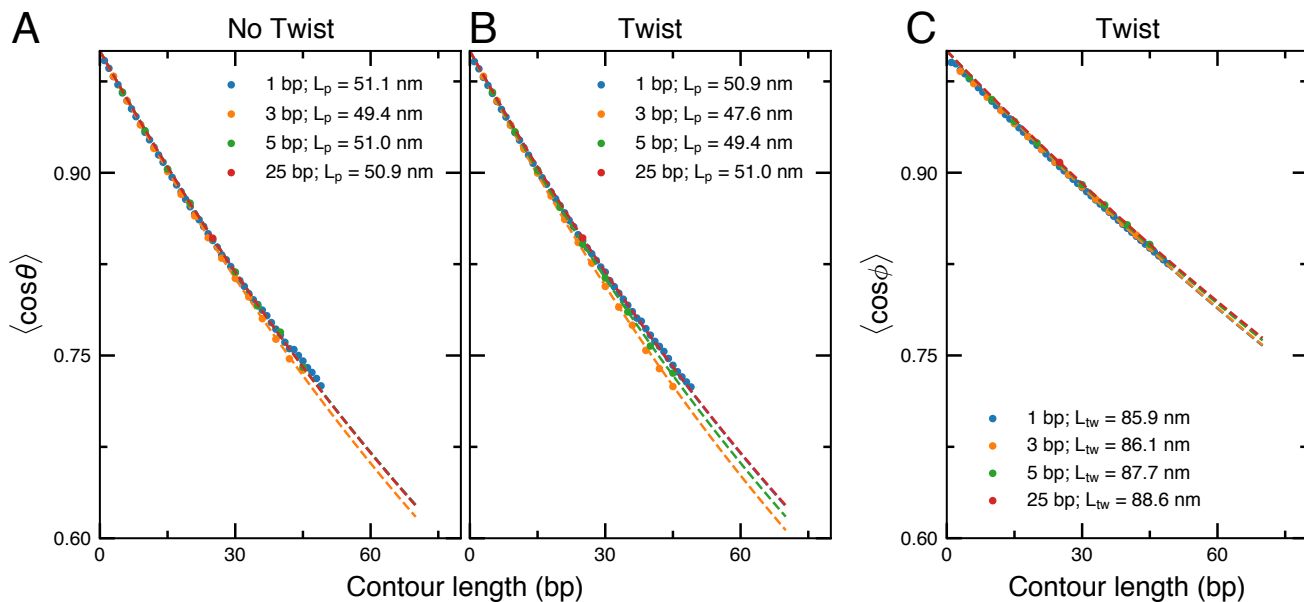


Figure S4: Polymer properties of the `mrdna` dsDNA model at different resolutions. (A,B) Contour-length dependence of the tangential correlations measured from `mrdna` simulations of a 300-bp dsDNA fragment at various resolutions lasting 500 million steps (40-fs timestep for 1-bp/dsDNA bead resolution; 150-fs otherwise), without (A) and with (B) a local representation of twist. Dashed lines depict exponentially decaying fits to the data, providing the persistence lengths of the DNA shown in the legend. (C) Contour-length dependence of the azimuthal correlation measured from the simulations described in panel B. Dashed lines depict exponentially decaying fits to the data, providing the twist persistence lengths of the DNA shown in the legend.

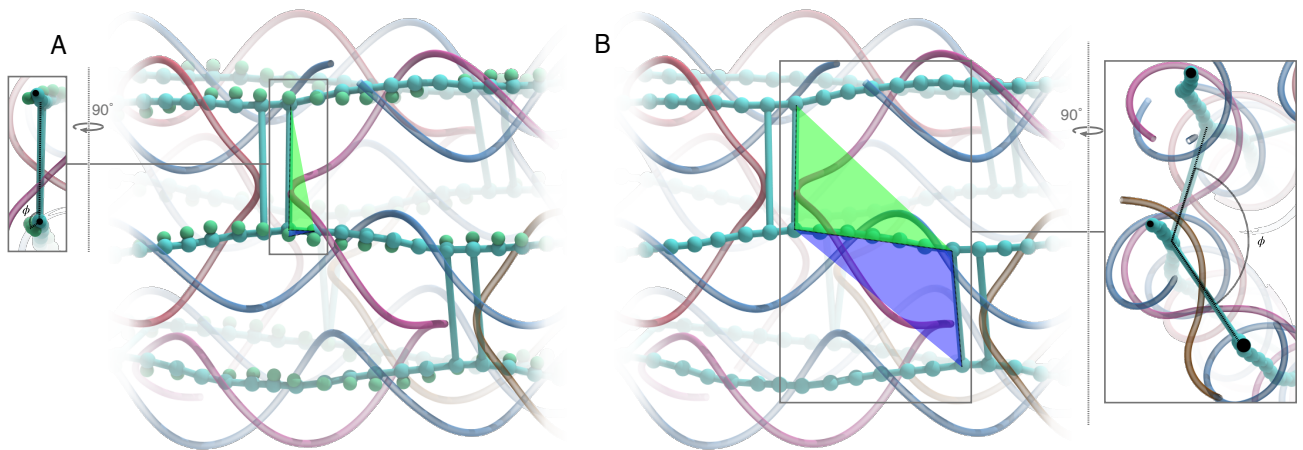


Figure S5: Twist in the `mrdna` dsDNA model around junctions. (A) Twist around dsDNA junctions when the model is constructed with a local representation of the DNA orientation. A harmonic potential is placed on the dihedral angle formed by two planes (green and blue in the figure) created by beads near the junction. The rest length is set to $\pm 120^\circ$ with the sign depending on the strand. (B) Twist around dsDNA junctions when the model is constructed without a local representation of the DNA orientation. A harmonic potential is placed on the dihedral angle formed by two planes (green and blue in the figure) created by beads forming consecutive pairs of junctions. The rest length is set to $s \times 34.48^\circ$, where s is the contour length between the junctions in basepairs; the spring constant is derived from the twist persistence length of DNA.

Supporting Code

Mrdna code for creating a model of the flask nanostructure

```
import numpy as np
from mrdna.readers import read_cadnano
from mrdna.coords import rotationAboutAxis
from mrdna.simulate import multiresolution_simulation as simulate

model = read_cadnano( "vase-44-final-ii-3.json" )

## Make crossovers at ends intrahelical
model.convert_crossovers_at_ends_beyond_cutoff_to_intrahelical(50)

## Rotate half flask by 90 degrees
c = model.get_center()
R = rotationAboutAxis( np.array((0,1,0)), -90 )
model.rotate(R,about=c, position_filter=lambda r: r[2] < c[2])

## Run the simulation
simulate( model = model,
          output_name = 'flask',
          directory = 'flask',
          gpu = 0,
          coarse_output_period = 1e5,
          fine_output_period = 1e3,
          coarse_steps = 1e7,
          fine_steps = 1e5,
        )
```

Mrdna code for creating a model of the gear nanostructure

```
import numpy as np
from mrdna.readers import read_cadnano
from mrdna.simulate import multiresolution_simulation as simulate
from mrdna.arbmodel.coords import rotationAboutAxis

filename = 'gear180.json'

model1 = read_cadnano( filename )
model2 = read_cadnano( filename )

## Transform model2, rotating it 180 degrees and shifting it 50 nm
R = rotationAboutAxis( axis=(1,0,0), angle=180 )
model2.rotate( R, about=model2.get_center() )
model2.translate( np.array((0,500,0)) )

## Functions to connect model1 and model2
def get_segments_in_vhelix( model, vhelix_idx ):
    """ Function for returning list of all mrdna segments
    corresponding to a a cadnano helix; segments are naturally ordered
    by increasing base index (left to right in cadnano window) """

    def segment_is_in_vhelix(seg):
        """ Mrdna naming convention for cadnano files is "i-j", where
```

```

        "i" is the virtual helix number, and "j" is a counter that
        increases as helices are added """

        seg_vhelix = seg.name.split('-')[0] # gets "i"
        return seg_vhelix == str(vhelix_idx)

    return [s for s in model.segments if segment_is_in_vhelix(s)]

def reconnect_ends(model1, model2):
    """ Special purpose function walks through all 18 cadnano helices
    in the main part of the gear, getting the last segment in the
    helix of one model and connecting it to the first helix in the
    other model """

    model1.convert_crossovers_at_ends_beyond_cutoff_to_intrahelical(50)
    model2.convert_crossovers_at_ends_beyond_cutoff_to_intrahelical(50)

    for i in range(18):
        s1 = get_segments_in_vhelix(model1, i)[-1]
        s2 = get_segments_in_vhelix(model2, i)[0]
        if (i % 2) == 0:
            s1.connect_end5(s2.start3)
        else:
            s1.connect_end3(s2.start5)

    for i in range(18):
        s1 = get_segments_in_vhelix(model2, i)[-1]
        s2 = get_segments_in_vhelix(model1, i)[0]

        if (i % 2) == 0:
            s2.connect_start3(s1.end5)
        else:
            s2.connect_start5(s1.end3)

    ## Combine models
    reconnect_ends(model1,model2)
    model1.extend(model2,copy=False)

    ## Run the simulation
    simulate(model1, output_name='2gear', directory='2gear',
             coarse_steps=1e7, fine_steps=1e5,
             coarse_output_period=1e5, fine_output_period=1e3,
    )

```


Supporting Animations

Animation 1: Movie illustrating the application of the `mrdna` framework for structure prediction of the pointer object⁶ to obtain an all-atom model. The structure is depicted using the same representations as Fig. 2 of the main text.

Animations 2-6: Comparison of average simulated structures and cryo-EM reconstructed densities of the pointer object⁶ (Animation 2); the v-brick structures without (Animation 3) and with the twist corrected (Animation 4);⁷ and the rectangular (Animation 5) and triangular (Animation 6) prisms for hierarchical assembly.⁷ Structures are depicted as in Fig. 3 of the main text.

Animations 7,8: Simulations of the flask object⁸ designed by the Yan group before (Animation 7) and after (Animation 8) breaking the symmetry of the flask in a Python script.

Animations 9-11: Depictions of structural fluctuations during 5-bp/bead resolution simulations of the caliper object from the Dietz group⁹ (Animation 9); the slider object from the Castro group;¹⁰ and the Bennett linkage object designed by the Castro group.¹¹

Animation 12: Electrostatic capture of a wireframe mesh nanostructure¹² in a nanopipette with a 300-mV applied bias.

References

- [1] Douglas, S. M.; Marblestone, A. H.; Teerapittayanon, S.; Vazquez, A.; Church, G. M.; Shih, W. M. *Nucleic Acids Res.* **2009**, *37*, 5001–6.
- [2] Rau, D. C.; Lee, B.; Parsegian, V. A. *Proc. Natl. Acad. Sci. U. S. A.* **1984**, *81*, 2621–2625.
- [3] Rothmund, P. W. K. *Nature* **2006**, *440*, 297–302.
- [4] Cocco, S.; Marko, J. F.; Monasson, R. *Biophysique* **2002**,
- [5] Mosconi, F.; Allemand, J. F.; Bensimon, D.; Croquette, V. *Phys. Rev. Lett.* **2009**, *102*, 078301.
- [6] Bai, X.-C. C.; Martin, T. G.; Scheres, S. H. W.; Dietz, H. *Proc. Natl. Acad. Sci. U. S. A.* **2012**, *109*, 20012–7.
- [7] Wagenbauer, K. F.; Sigl, C.; Dietz, H. *Nature* **2017**, *552*, 78.
- [8] Han, D.; Pal, S.; Nangreave, J.; Deng, Z.; Liu, Y.; Yan, H. *Science* **2011**, *332*, 342–6.
- [9] Funke, J. J.; Ketterer, P.; Lieleg, C.; Korber, P.; Dietz, H. *Nano Lett.* **2016**, *16*, 7891–7898.
- [10] Marras, A.; Zhou, L.; Kolliopoulos, V.; Su, H.; Castro, C. *New J. Phys.* **2016**, *18*, 055005.
- [11] Marras, A. E.; Zhou, L.; Su, H.-J.; Castro, C. E. *Proc. Natl. Acad. Sci. U. S. A.* **2015**, *112*, 713–718.
- [12] Benson, E.; Mohammed, A.; Gardell, J.; Masich, S.; Czeizler, E.; Orponen, P.; Högberg, B. *Nature* **2015**, *523*, 441–444.